

INVERSION OF THICK-TARGET BREMSSTRAHLUNG SPECTRA FROM NONUNIFORMLY IONISED PLASMAS

JOHN C. BROWN¹, GUILLIAN K. MCARTHUR¹, RICHARD K. BARRETT¹,
SCOTT W. MCINTOSH¹ and A. GORDON EMSLIE²

¹*Department of Physics and Astronomy, University of Glasgow, G12 8QQ, U.K.*

²*Department of Physics, The University of Alabama in Huntsville, AL 35899, U.S.A.*

(Received 9 June 1997; accepted 22 October 1997)

Abstract. The effects of non-uniform plasma target ionisation on the spectrum of thick-target HXR bremsstrahlung from a non-thermal electron beam are analysed. In particular the effect of the target ionisation structure on beam collisional energy losses, and hence on inversion of an observed photon spectrum to yield the electron injection spectrum, is considered and results compared with those obtained under the usual assumption of a fully ionised target.

The problem is formulated and solved in principle for a general target ionisation structure, then discussed in detail for the case of a step function distribution of ionisation with column depth as an approximation to the sharp coronal–chromospheric step structure in solar flare plasmas. It is found that such ionisation structure has very dramatic effects on derivation of the thick-target electron injection spectrum $F_0(E_0)$ as compared with the result $F_0^*(E_0)$ obtained under the usual assumption of a fully ionised target: (a) Inferred F_0^* contain more electrons than F_0 and in some cases include electrons at energies where none are actually present. Although the total (energy-integrated) beam fluxes in the two cases do not differ by a factor of more than $\Lambda_{ee}/\Lambda_{eH}$, the spectral shapes can differ greatly over finite energy intervals resulting in the danger of misleading results for total fluxes obtained by extrapolation. (b) The unconstrained mathematical solution for F_0 for any photon spectrum is never unique, while that for F_0^* is unique. When the physical constraint $F_0 \geq 0$ is added, for some photon spectra solutions for F_0 may not exist or may not be unique. (This is *not* an effect of noise but of real analytic ambiguity.) (c) For data corresponding to F_0^* with a low-energy cut-off, or a cut-off or rapid enough exponential decline at high energies, a unique solution F_0 does exist and we obtain a recursive summation for its evaluation.

Consequently, in future work on the inversion of HXR bremsstrahlung spectra it will be vital for algorithms to include the effects of target ionisation if spurious results on thick-target electron spectra are not to be inferred. Finally it is pointed out that the depth of the transition zone, and its evaporative evolution during flares may be derivable from its effect on the HXR spectrum.

1. Introduction

Inferring the flux spectrum of energetic electrons accelerated during the solar flare is of fundamental importance in flare theory, both insofar as it is a signature of the acceleration process and also since such electrons probably carry a large fraction of the impulsive phase power. Brown (1971, 1975) pointed out that the inference of the electron spectrum from HXR bremsstrahlung is an integral inverse problem and obtained solutions (for the Kramer's and Bethe–Heitler cross-sections) in both thin- and thick-target cases for a uniformly ionised background plasma. Such an inverse approach remained of largely academic interest until the advent of Ge detector spectrometry (Lin and Schwartz, 1987), the resolution of which is high compared to the typical 'width' of HXR spectra, so providing spectra which can be

inverted, subject to the limitations imposed by data noise and the intrinsic instability of the inversion, to yield the electron spectrum. Numerical schemes to conduct the inversion, with explicit or implicit smoothing to suppress the instability, have consequently been carried out by Johns and Lin (1992), Thompson *et al.* (1992), and Piana (1994).

In addition to the effects of data noise, the solution for the electron spectrum is influenced by the bremsstrahlung cross-section used (Brown and Emslie, 1988), by bremsstrahlung directivity effects (e.g., MacKinnon and Brown, 1989), photospheric albedo considerations at low energies (Tomblin, 1972; Santangelo *et al.*, 1973), and by non-uniform energy loss processes in the source (Brown and MacKinnon, 1985). All of these can be loosely regarded as ‘perturbations’ of the kernel function of the integral inverse problem. Such ‘perturbations’ can, in some cases, seriously affect the solution (Judge, Hubeny, and Brown, 1997), partly because they introduce an error that, like data errors, can be amplified by the instability or ill-posedness of the inverse operator, but also, and more crucially, because they change the structure of the inversion and can lead to ill-posedness in regimes where none existed before. In this paper we consider one of these effects – non-uniform ionisation of a thick-target source and its effects on the electron energy losses – and its consequences for the bremsstrahlung inversion problem, to see whether it seriously affects the form of inferred electron spectra and how it can be incorporated in inference algorithms.

Brown (1973) pointed out that reduction of collisional energy losses of electrons in a weakly ionized plasma, as compared to a fully ionized one, affects the relation between the HXR bremsstrahlung spectrum and the electron spectrum at injection in a solar flare thick-target model. This is because the bremsstrahlung efficiency (the fraction of electron energy going into direct radiation rather than collisional plasma heating) is higher for more energetic electrons which penetrate from the corona into the chromospheric regions of low ionisation, where Coulomb energy losses are reduced. In that paper Brown computed the HXR spectrum from such a beam for the case of a power-law injection spectrum, and showed that the HXR spectral slope should flatten at intermediate energies, compared to the power law HXR spectrum predicted for a uniformly ionized target.

The consequences of this non-uniform ionisation effect on thick-target HXR spectra has never been followed up in the literature and, in particular, the corresponding inverse problem has never been addressed. That is, for a *given* observed HXR spectrum, what is the effect of non-uniform target ionisation on the inferred thick-target electron spectrum? Here we formulate this problem for a general form of ionisation distribution and study its inversion properties for a special but realistic case of ionisation structure. The fact that the effect in the forward problem is modest and smooth might lead us to suppose naively that the same would be true of the inverse problem. Nothing could be further from the truth, as we will show.

2. Formulation of the Problem

Following Brown (1972, 1973) and Emslie (1978), we consider electrons descending a vertical magnetic field along which the total (free and bound) electron column density $N(\text{cm}^{-2})$ from the injection site is a central parameter in the collisional transport problem. For simplicity we consider the approximation where only energy loss is considered and neglect pitch-angle changes since we are going to neglect directivity effects in the emission and concentrate only on *relative* changes in the spectrum arising from target ionisation variations. Then, in a hydrogen target of ionisation level $x(N)$ at depth N the electron energy E equation is

$$\frac{dE}{dN} = -\frac{2\pi e^4 \Lambda}{E} [\lambda + x(N)], \quad (1)$$

where $\Lambda = \Lambda_{ee} - \Lambda_{eH}$, $\lambda = \Lambda_{eH}/\Lambda \approx 0.55$ with Λ_{ee} and Λ_{eH} the Coulomb logarithms for electron–electron and electron–H collisions.

Then the thick-target bremsstrahlung photon emission rate per unit photon energy ϵ , for electron injection rate $F_0(E_0)$ per unit injection energy E_0 , is

$$J(\epsilon) = \frac{Q_0}{K\epsilon} \int_{\epsilon}^{\infty} F_0(E_0) \int_{\epsilon}^{E_0} \frac{q(\epsilon, E) dE dE_0}{\lambda + x(E, E_0)}, \quad (2)$$

where $K = 2\pi e^4 \Lambda$, the bremsstrahlung cross-section differential in ϵ has been written as $q(\epsilon, E)Q_0/\epsilon E$ with Q_0 a constant, and $x(E, E_0)$ is the value of $x(N)$ at the depth N where an electron of injection energy E_0 has slowed to energy E as described by the solution of Equation (1),

$$E_0^2 - E^2 = 2KM,$$

where

$$M(N) = \int_0^N (\lambda + x(N')) dN'$$

is an ‘effective’ collisional column density. Since $M(N)$ is monotonic we can rewrite $x = x(M = (E_0^2 - E^2)/2K)$ and compute it for any model atmosphere so that Equation (2) becomes

$$H(\epsilon) = \frac{K\epsilon}{Q_0} J(\epsilon) = \int_{\epsilon}^{\infty} F_0(E_0) \int_{\epsilon}^{E_0} \frac{q(\epsilon, E) dE dE_0}{\lambda + x\left(\frac{E_0^2 - E^2}{2K}\right)}. \quad (3)$$

Here we will assume $q(\epsilon, E) = 1$, i.e., Kramer's cross-section, to be an adequate approximation for describing the relative effects of $x(M)$ on the relation between $H(\epsilon)$ and $F_0(E_0)$. In this case, reversing the integrals and differentiating with respect to ϵ yields

$$\int_{\epsilon}^{\infty} F_0(E_0) k(E_0^2 - \epsilon^2) dE_0 = -H'(\epsilon) = L(\epsilon), \quad (4)$$

where

$$k(E_0^2 - \epsilon^2) = \frac{1}{\lambda + x \left(\frac{(E_0^2 - \epsilon^2)}{2K} \right)}. \quad (5)$$

This is an integral equation for $F_0(E_0)$ to be solved for given data $H(\epsilon)$ and for the kernel function k defined by $x(M)$ in a model target atmosphere. Choosing some convenient characteristic energy E_1 , defining $\xi = \epsilon^2/E_1^2$, $\eta = E_0^2/E_1^2$, $f(\eta)d\eta = F_0(E_0)/F_1 dE_0$, $g(\xi) = L(\epsilon)/L_1$, where $L_1 = L(E_1)$, $F_1 = F_0(E_1)$, and renaming $k(E_0^2 - \epsilon^2) = k(\eta - \xi)$, we obtain

$$\int_{\xi}^{\infty} f(\eta) k(\eta - \xi) d\eta = g(\xi) = \frac{1}{\lambda + 1} \int_{\xi}^{\infty} f^*(\eta) d\eta, \quad (6)$$

where $f^*(\eta)$ is the solution for a fully ionized target (Equations (3) and (4) with $x = 1$) usually used in HXR spectral analysis. Equation (6) is of general convolution form with kernel $k(\zeta) = 0$ for $\zeta < 0$ and so can in principle be solved (cf., Craig and Brown, 1986) by a variety of standard methods including Fourier transform for any kernel function k specified by $x(M)$. This thick-target spectral inversion problem can then be seen as a generalisation of that considered by Brown (1971) and Johns and Lin (1992) for a uniformly ionized target. In the following we consider the effect of non-uniform ionisation on the solution for the electron spectrum function $f(\eta)$ for one idealized form of k , i.e., of the ionisation level $x(M)$, deferring more general cases to a subsequent paper.

3. Solution for Step Function Ionisation

Hydrogen ionisation in the solar atmosphere falls sharply with M across the transition zone. In simplified form this can be approximated as $x = 1$ for $M \leq M_1$, $x = 0$ for $M > M_1$, where $M_1 = (\lambda + 1)N_1$ and N_1 is the column density between the acceleration site and the transition zone. If we use $x = x_0$ with $0 < x_0 < 1$ instead of $x = 0$ for $M > M_1$ the following analysis and its alarming consequences

still hold but with λ^{-1} replaced by $1/(\lambda + x_0)$ in Equation (7) for $\xi > 1$. We argue in Section 7 that smoothing of the sharp ionisation step used in (7) does not change our main conclusions. Using $E_1 = (2KM_1)^{1/2}$ as the characteristic energy here (so that η is E_0^2 in units of the E_0 value = E_1 required to just reach the transition zone) then

$$k(\zeta) = \begin{cases} \frac{1}{(\lambda + 1)} & \zeta < 1, \\ \frac{1}{\lambda} & \zeta > 1, \end{cases} \quad (7)$$

and (6) becomes

$$\frac{1}{(\lambda + 1)} \int_{\xi}^{\xi+1} f(\eta) \, d\eta + \frac{1}{\lambda} \int_{\xi+1}^{\infty} f(\eta) \, d\eta = g(\xi),$$

which, on differentiation with respect to ξ , reduces to the non-integral form

$$f(\eta) + \nu f(\eta + 1) = -(\lambda + 1)g'(\eta) = f^*(\eta), \quad (8)$$

where ν is defined as (λ^{-1}) , to be solved for $f(\eta)$ given data $g(\xi)$ or, equivalently, given $f^*(\eta)$ (though $f^*(\eta)$ will of course be much noisier than $g(\xi)$ in real cases). Note that $\nu = \lambda^{-1} = (\Lambda_{ee}/\Lambda_{eH} - 1) > 1$.

4. The Forward Problem

Equation (8) can be used in several ways explore the differences between the electron injection spectra required to produce a prescribed photon spectrum for the cases of fully and step-function ionized targets. It is informative to start with solution of the forward problem – i.e., evaluation of the injection spectrum $f^*(\eta)$, (corresponding to $F_0^*(E_0)$), which would have to be used in a wholly ionized target to yield the same photon spectrum $J(\epsilon)$ as actually produced by injection of spectrum $f(\eta)$, ($F_0(E_0)$), into a target with an ionisation discontinuity at depth $M_1 = (E_1^2/2K)$. Equation (8) shows that $f^*(\eta)$ is characterized by a ‘primary’ component identical to $f(\eta)$, plus a ‘secondary’ component proportional to $f(\eta + 1)$. The simplest example of this is the case of a single narrow spike form for f which we describe as

$$f(\eta) = \delta(\eta - \eta_s),$$

with δ the delta function, for which Equation (8) implies

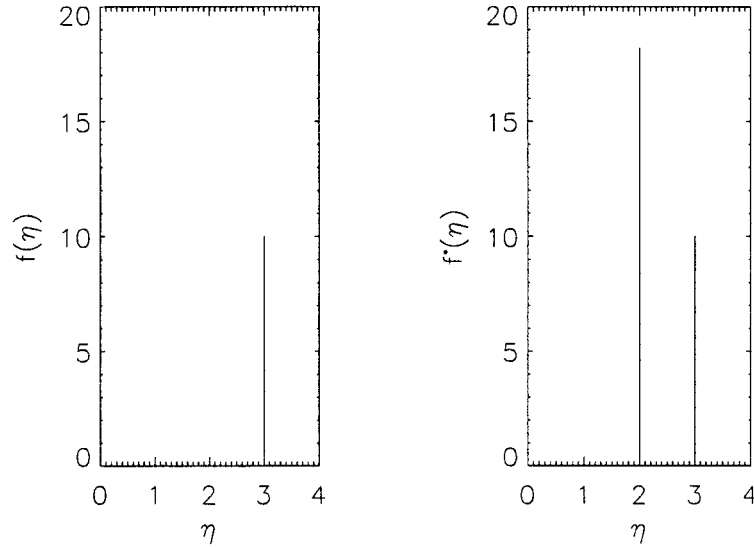


Figure 1. Injection spectrum f^* required for an ionized target to yield the same photon spectrum as a single-spike (δ -function) spectrum f injected into a step-function-ionized target.

$$f^*(\eta) = \delta(\eta - \eta_s) + \nu\delta(\eta - (\eta_s - 1))$$

shown in Figure 1 for $\eta_s = 3$. It follows that to produce the same thick-target bremsstrahlung spectrum as monoenergetic electrons (energy E_{0s}) injected into a step-function-ionized target such as the Sun, a fully-ionized target would need injection of two distinct monoenergetic electron components of energies E_{0s} and $(E_{0s}^2 - E_1^2)^{1/2}$. (Here we have assumed that $\eta_s > 1$. If $\eta_s < 1$ all electrons stop in the corona and $f^* \equiv f$.) Physically the reason for the additional ‘secondary’ component is that in the real (step-function-ionized) target some of the low-energy photons are produced at higher efficiency (ratio $\Lambda_{ee}/\Lambda_{eH} = \nu + 1$) by electrons that reach the unionized region. For a fully ionized target to reproduce this demands addition of an extra flux of electrons $([\nu + 1] - 1 = \nu$ times as large as the original flux) at energies equal to $(E_{0s}^2 - E_1^2)^{1/2}$, the energy at which the electrons in the actual target first encounter a neutral medium (see Figure 2). This simple explanation for the δ -function case shows that our general results below are in fact independent of the precise form of the bremsstrahlung cross-section $q(\epsilon, E)$ used.

We next examine some examples of $f(\eta)$ which are smooth (continuous) and monotonic. The simplest case is that form of $f(\eta)$ which is shape preserving under η translation – i.e., $f(\eta + 1) = af(\eta)$, where a is a constant, that form being $f = e^{\beta\eta}$, where $a = e^\beta$. Substitution in Equation (8) gives the corresponding

$$f^*(\eta) = (1 + \nu e^\beta)e^{\beta\eta} = (1 + \nu e^\beta)f(\eta).$$

Thus all exponential spectra (exponential in $\eta = E_0^2/E_1^2$, not in E_0) preserve shape under functional operation (8), $f^*(\eta)$ differing from $f(\eta)$ only by a constant factor.

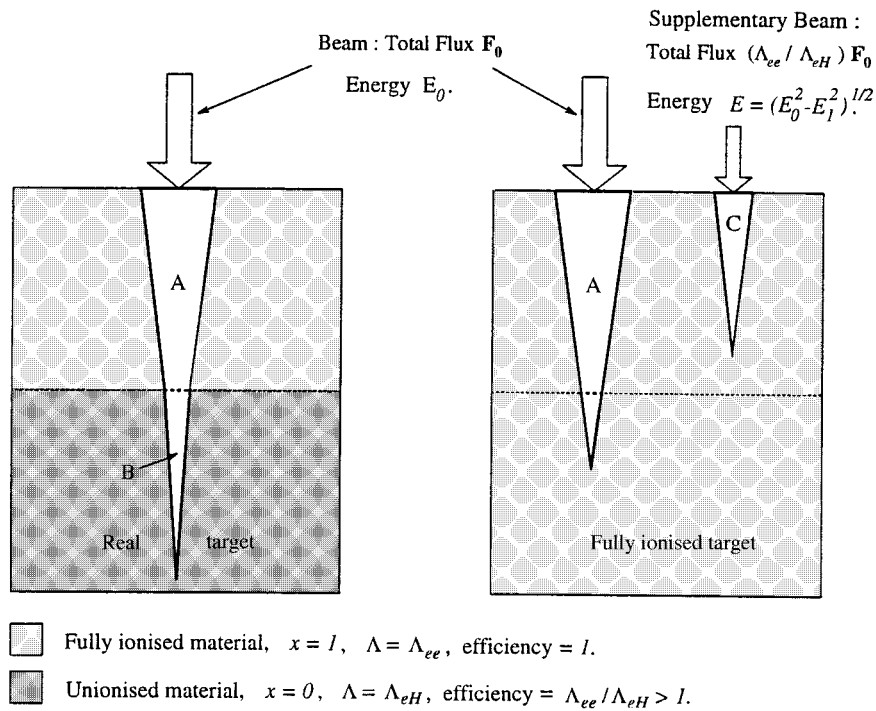


Figure 2. Injection of an electron beam of total flux F_0 and energy E_0 into a target with step function ionisation (left panel) produces bremsstrahlung in the upper ionized target with ‘efficiency’ 1, then enters the lower target as a beam of flux F_0 at energy $(E_0 - E_1^2)^{1/2}$, where it produces bremsstrahlung with efficiency $\Lambda_{ee} / \Lambda_{eH}$. Injection of the same initial beam alone into an ionized target (right panel) produces less bremsstrahlung by an amount equal to that from a beam of energy $(E_0 - E_1^2)^{1/2}$ and flux $(\Lambda_{ee} / \Lambda_{eH} - 1)F_0$. To match the bremsstrahlung from the left panel, therefore, an ionized target requires the injection of a supplementary beam with these parameters.

This is true whether $\beta = 0$ (completely flat spectrum), $\beta < 0$, $\beta > 0$ or β complex so that harmonic components are present. (However, cases $\text{Re}[\beta] > 0$ are physical only if there is an upper cut-off in which case the translation invariance property breaks down). In the case of complex β the shape, including harmonic variation, is preserved though in general with a phase shift as well as an amplitude change. As an example we show in Figure 3 the forms of f , f^* for

$$f(\eta) = A + Be^{(C+i\omega)\eta}$$

with $A = 2$, $B = 1$, $C = \frac{1}{3}$, $\omega = 10$, where we have added a constant term A so that $f(\eta) > 0$. In this case the translation is of the form $f^* = a_1 + a_2 f(\eta)$, still shape-preserving but no longer simply scalar.

Shape preservation does not occur for other forms of f . For a single power-law form $f(\eta) = \eta^{-\alpha}$ at all η (where $\alpha = (\delta + 1)/2$, with δ the corresponding index for $F_0(E_0)$), the corresponding f^* is the sum of a power law and a shifted power law:

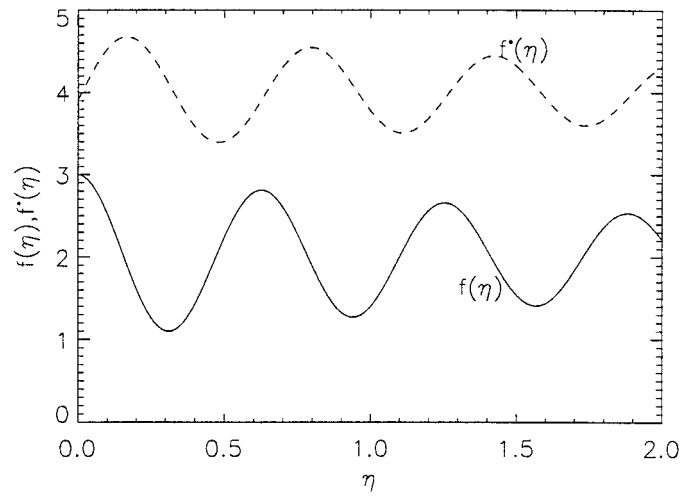


Figure 3. Injection spectrum f^* required for an ionized target to yield the same photon spectrum as an exponential/harmonic spectrum f injected into a step-function-ionized target.

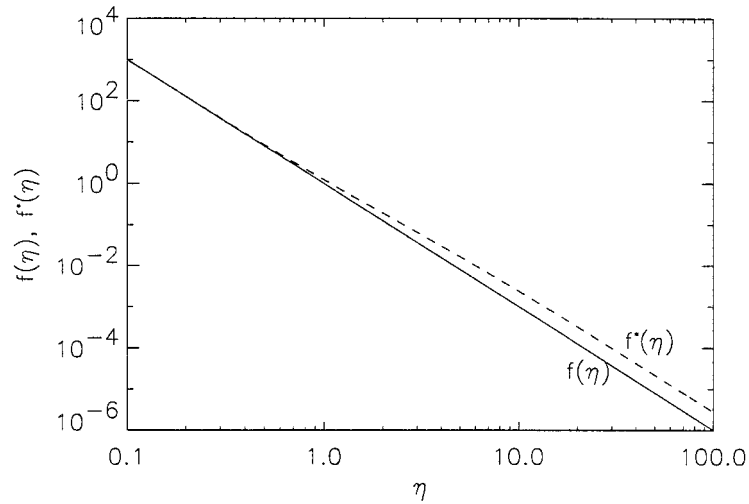


Figure 4. Injection spectrum f^* required for an ionized target to yield the same photon spectrum as a pure power-law spectrum f injected into a step-function-ionized target.

$$f^*(\eta) = \eta^{-\alpha} + \nu(\eta + 1)^{-\alpha}$$

which is shown in Figure 4 for $\alpha = 3$ ($\delta = 5$). This is essentially the same as the result of Brown (1973) except that here we show the form of f^* rather than of the photon spectrum. For this case the difference between $f(\eta)$ and $f^*(\eta)$ is appreciable in scale (factors of up to $1 + \nu$) but not dramatic in shape, especially in a $(\log f, \log \eta)$ plot. As in all integral problems, however, the most striking effects occur for source functions with sharp features rather than for smooth ones like unbroken power laws.

For example, if $f(\eta)$ is non-zero over the range $\eta_1 < \eta < \eta_2$ then by Equation (8) $f^*(\eta)$ is non-zero over the ranges $\eta_1 < \eta < \eta_2$ and $\eta_1 - 1 < \eta < \eta_2 - 1$ which overlap if $\eta_1 < \eta_2 - 1$. This is shown in Figures 5(a) and 5(b) for $f(\eta) = 1$ in $1 < \eta < 1.5$, and in $1 < \eta < 3$, respectively. For the case of a power law with low cut-off at $\eta = \eta_1$ we obtain the results in Figures 6(a) and 6(b) for $\eta_1 = 0.5, 1.5$ for power-law index $\alpha = 3$. In general we see, from the forward problem, that in order to yield a given photon spectrum for a fully ionized target it is necessary to enhance the number of electrons everywhere compared to the electron injection spectrum needed for a step-function-ionized target, sometimes including addition of electrons in ranges of η (i.e., of energy) where none were previously required. The double-peaked f^* arising from a single f can be seen as a generalisation of our discussion of the delta function f above. The spurious introduction of these extra electrons, by inversion of a bremsstrahlung spectrum using an erroneous, fully ionized, target model, will result in incorrect conclusions concerning the electron acceleration mechanism insofar as this determines the spectral shape. It may also significantly affect inference of total electron beam power in flares, particularly if the inferred spectrum is extrapolated, using the wrong spectral shape, outside the range in which it is directly inferred from HXR data, as is often done (cf., Brown, 1971).

In reality it is not $f(\eta)$, $F_0(E_0)$ which is given but rather the photon data $J(\epsilon)$ which, in the idealised case of low enough data noise to allow determination of $g'(\eta)$ by differentiating twice, yields from (8) the form of the (hypothetical) $f^*(\eta)$ needed to produce it. Thus, in terms of data interpretation, what we are really interested in is the inverse solution of (8) for $f(\eta)$ given $f^*(\eta)$, rather than the converse. This turns out to be a less simple issue.

5. The Inverse Problem

5.1. NONUNIQUENESS OF THE UNCONSTRAINED MATHEMATICAL SOLUTION

The inverse problem of determining the injection spectrum required for a realistic step-function-ionized target from the observed HXR spectrum amounts to solving Equation (8) for $f(\eta)$ for a given $f^*(\eta)$. Though seemingly innocuous, (involving no integration for example), this is not a simple problem, involving solution of a so-called functional equation. For such equations conditions for existence and uniqueness of solutions are far from trivial to arrive at and the literature on them very sparse (cf., Kuczma, 1968). Here we explore the main facets of the functional equation (8) most relevant to the issue in hand. (We do so here purely for 'perfect' data for which the noise, resolution, and bandwidth are good enough to define f^* accurately, but we recognise that noise, discretisation and truncation in f^* will in practice affect our conclusions. For example, a physically acceptable (non-negative) solution may not exist for f for some data realisation f^* , but one or more may

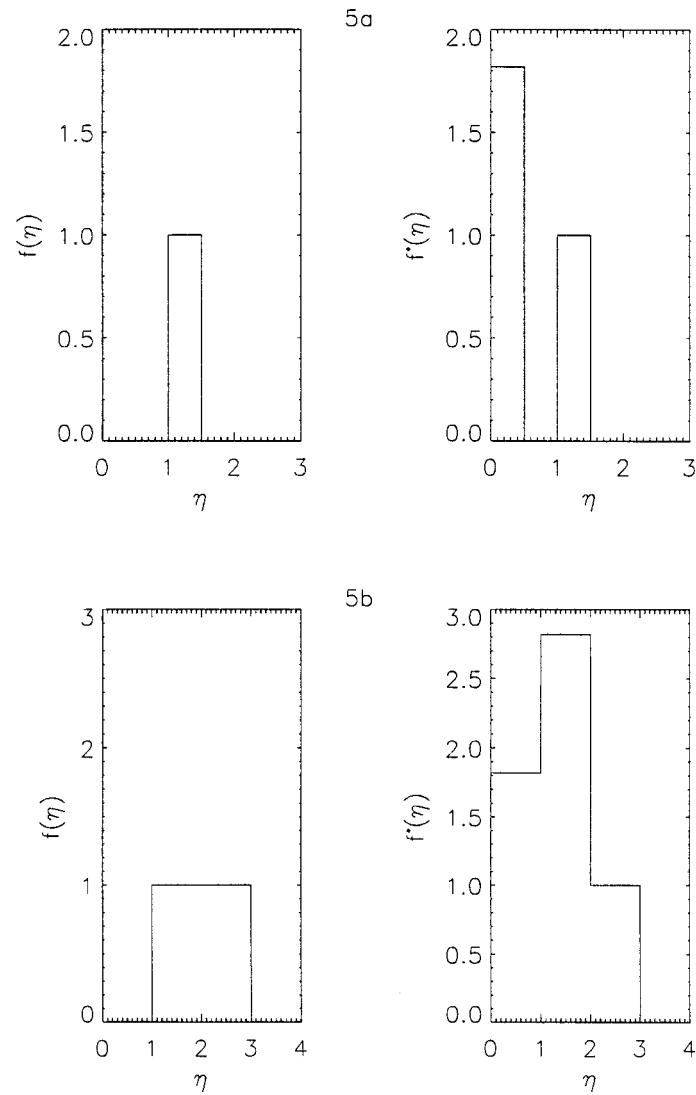


Figure 5. Injection spectrum f^* required for an ionised target to yield the same photon spectrum as a 'top-hat' spectrum f injected into a step-function-ionized target, for two different 'top-hat' locations. (a) For $f(\eta) = 1$ in $1 < \eta < 1.5$. (b) For $f(\eta) = 1$ in $1 < \eta < 3$.

exist for alternative data realisations within the error bounds of f^* . Treatment of this issue will require use of regularisation or other smoothing methods of solving the inverse problem.)

A simple example is when the photon spectrum observed corresponds to that from a single spike injected into a fully ionized target, i.e., $f^* = \delta(\eta_1)$. Then if $\eta_1 = m + \Delta m$, where m is integer and $0 < \Delta m < 1$, for f to be physical we

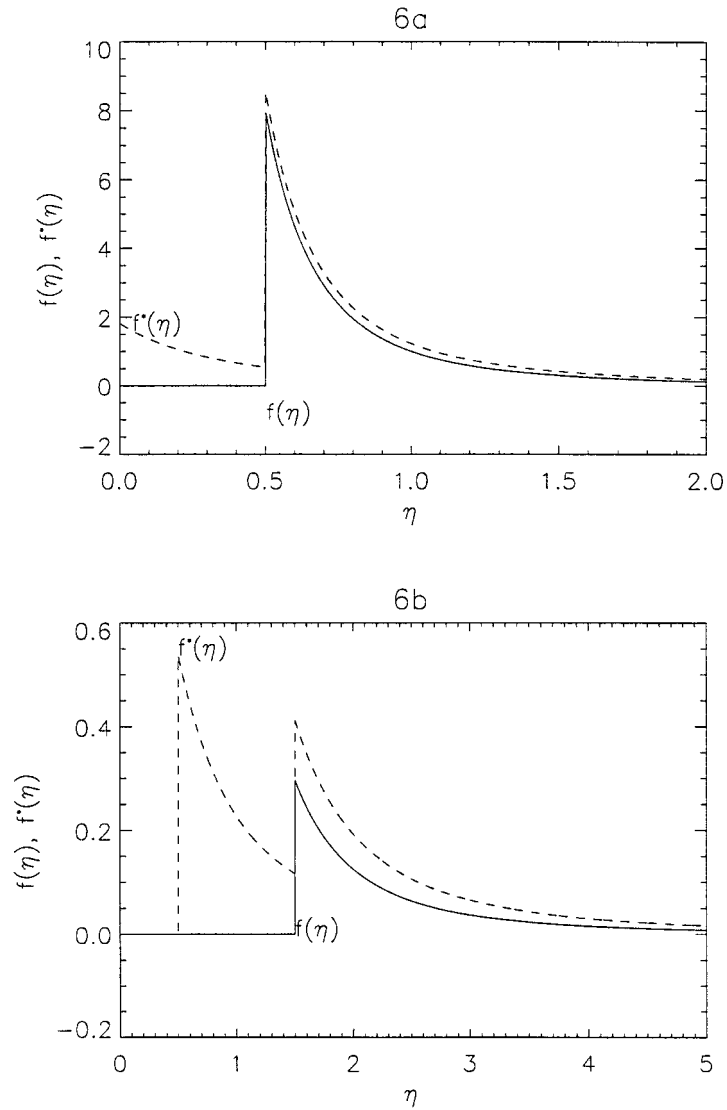


Figure 6. Injection spectrum f^* required for an ionized target to yield the same photon spectrum as a power-law spectrum f with low cut-off injected into a step-function-ionized target, for two different cut-off values.

require $f(\eta) = 0$ for $\eta > \eta_1$ and hence $f(\eta_1) = f^*(\eta_1)$. It is easy then to show from Equation (8) that

$$f(\eta) = \sum_{i=0}^m (-\nu)^i \delta(\eta - \eta_1 - i), \tag{9}$$

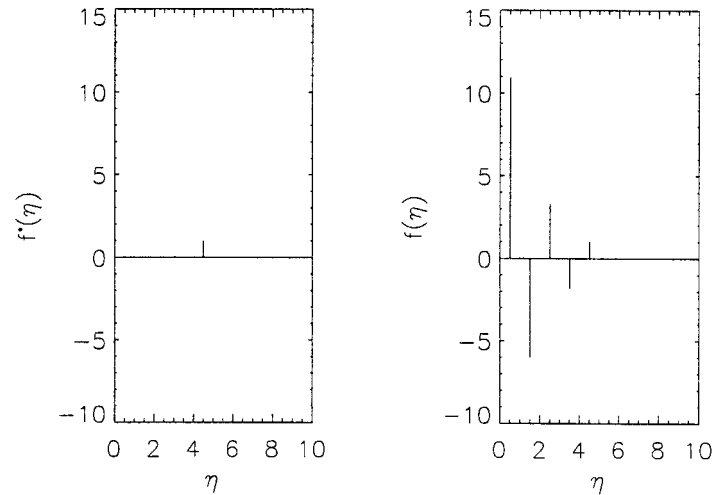


Figure 7. Injection spectrum f required for a step-function-ionized target to yield the same photon spectrum as a single spike (δ -function) spectrum f^* injected into an ionized target.

illustrated in Figure 7 for $\eta_1 = 4.5$. Here each ‘primary’ contribution to $f^*(\eta)$ from the δ -function at $\eta = \eta_1 - 1$ in $f(\eta)$ cancels the ‘secondary’ contribution to $f^*(\eta)$ from the δ -function at $\eta = \eta_1$. The δ -function at $\eta_1 = 0.5$ has no ‘secondary’ component (since all the electrons stop in the ionized corona), therefore no additional ‘primary’ components are required and the series of δ -functions in $f(\eta)$ is finite. Thus, unless $\eta_1 < 1$ the formal solution for f for a δ -function f^* comprises a geometric series of δ -function amplitudes of alternating signs, separated by intervals of 1 in η , which is completely unphysical. Note also that since $\nu > 1$ the amplitude of the series of δ -function components increases geometrically (factor $(-\nu)$ – Equation (9)) with decreasing η until the sequence terminates at the first $\eta < 1$. If ν were less than unity (e.g., if the ionisation level in the chromosphere were $x_0 > x_{\text{crit}}$, where $(\lambda + 1)/(\lambda + x_{\text{crit}}) = 2$, i.e., $x_{\text{crit}} \geq 0.225$ here), then the size of the δ -functions would decrease with decreasing η . Also, if ν were *negative* (corresponding to the injection of electrons into a target with an *upward* step in ionisation level), then the solution of (9) would be a series of *non-alternating* δ -functions. (Physically, the decreased efficiency in the second part of the target in this case means that we have to add electrons at lower energies to produce the same spectrum as in a uniform ionisation target. These electrons in turn produce bremsstrahlung, requiring additional electrons at lower energies to compensate for the reduced efficiency in the second part of the target, etc., until the last ‘addition’ stops entirely in the first part of the target.)

Now we obtain the important result that, without imposing prior conditions (i.e., conditions from outwith the equation itself) on f , the solution of Equation (8) for f can never be unique for any f^* . By contrast, the solution of the problem for the fully ionized case is unique, viz., $f = f^* = -(\lambda + 1)g'(\eta)$ – though we require

$g'(\eta) < 0$ in order to satisfy the *a priori* physical condition $f \geq 0$ (Brown and Emslie, 1988). The same is true for a target with any uniform level of ionisation. To see the non-uniqueness we note that to any solution f of Equation (8) can be added another solution f_0 of the homogeneous form of Equation (8):

$$f_0(\eta + 1) = -\lambda f_0(\eta) . \quad (10)$$

The above is not an equation for f_0 but only a recursion relation expressing $f_0(\eta + 1)$ in terms of $f_0(\eta)$. Thus f_0 can have any functional form whatsoever in, e.g., the interval $0 < \eta \leq 1$, say $f_0(\eta) = \phi(\eta)$, and in interval $(\eta + j, \eta + j + 1)$ it is

$$f_0(\eta + j) = (-\lambda)^j \phi(\eta) . \quad (11)$$

This can be written $f_0(\eta) = (-\lambda)^j \phi(\eta_0)$, where j is the largest integer strictly less than η ($j < \eta$) and η_0 is defined by $\eta = j + \eta_0$, so that $0 < \eta_0 \leq 1$. This notation will be used frequently in what follows. Such functions f_0 belong to the null space of the operator defining functional Equation (8), i.e., they contribute nothing to the data $f^*(\eta)$, and addition of any arbitrary combination of them cannot be excluded without use of prior assumptions on f such as based on physical acceptability. That is, if some function $f_1(\eta)$ satisfies Equation (8) then so does $f_1(\eta) + (-\lambda)^j \phi(\eta_0)$ (again with $\eta = \eta_0 + j$) for any function $\phi(\eta_0)$ whatsoever defined on $(0, 1]$. *So, without physical constraints there exist an infinity of solutions to the thick-target bremsstrahlung inversion problem for a step-function ionized target.* In terms of physical intuition this is rather alarming. Since it will remain true for any $x = x_0 \neq 1$, this means that an infinity of solutions exist for any finite step in ionisation unless we add additional (non-spectral) information to the problem.

5.2. PHYSICALLY ACCEPTABLE SOLUTIONS

We now consider the existence and uniqueness of solutions to Equation (8) when physical constraints are applied to $f(\eta)$. These could include, for example, continuity, but this is too restrictive since real electron spectra could very well possess discontinuities. Indeed such electron spectra may be of particular physical interest. We therefore restrict ourselves to the most liberal possible restrictions on $f(\eta)$, namely that $f(\eta) \geq 0$ and that $f(\eta)$ is bounded. We also note that we should restrict $f(\eta)$ such that the total electron beam flux and power should be finite. This requires that $f(\eta) \rightarrow 0$ as $\eta \rightarrow \infty$ faster than $\eta^{-3/2}$ and that $f(\eta) \rightarrow \infty$ as $\eta \rightarrow 0$ slower than η^{-1} . The latter formal condition, which is not in fact met for typical HXR spectra in their observed range, is complicated by the low-energy masking effects of the thermal bremsstrahlung contribution (Lin and Schwartz, 1987).

We focus attention first on the requirement that $f(\eta) \geq 0$ and introduce the other conditions later. If a solution of Equation (8) exists and is $f(\eta) = \phi(\eta)$ in some interval $\eta_1 < \eta \leq \eta_1 + 1$, which we will choose without loss of generality to be $0 < \eta \leq 1$, then we can obtain the solution over the whole range by noting that in $1 < \eta \leq 2$

$$f(\eta) = \lambda[f^*(\eta - 1) - \phi(\eta - 1)]$$

and by recursive use of this argument we have

$$f(\eta_0 + j) = (-\lambda)^j \left[\phi(\eta_0) - \sum_{i=0}^{j-1} (-\nu)^i f^*(\eta_0 + i) \right], \quad (12)$$

where $\eta = \eta_0 + j$ with j integer and $0 < \eta_0 < 1$.

Physically we require $f(\eta) \geq 0$ for all j and all $0 < \eta_0 \leq 1$ for which Equation (12) requires

$$\sum_{i=0}^{2k-1} (-\nu)^i f^*(\eta_0 + i) \leq \phi(\eta_0) \leq \sum_{i=0}^{2k} (-\nu)^i f^*(\eta_0 + i) \quad (13)$$

for all $k \geq 0$ and all $0 < \eta_0 \leq 1$, where we have introduced k to distinguish even $j = 2k$ and odd $j = 2k + 1$ to deal with the opposite signs of the inequality for even and odd j . From Equation (13) it follows that $\phi(\eta_0)$ is unique if the sums in (13) converge absolutely, i.e., if

$$S(\eta_0) = \sum_{i=0}^{\infty} |(-\nu)^i f^*(\eta_0 + i)| = \sum_{i=0}^{\infty} \nu^i f^*(\eta_0 + i) \quad (14)$$

converges. (This condition is sufficient, but not necessary: uniqueness can occur without Equation (14) being satisfied in some circumstances.)

If $|\nu| < 1$ the series converges. $|\nu| < 1$ corresponds to $0 < \Lambda_1/\Lambda_2 < 2$, i.e., cases where the ionisation fraction either increases with depth or decreases to a specific value > 0 (e.g., 0.225 if the upper target is fully ionized). In such cases, convergence would be guaranteed for bounded f . But for the present case of $\nu > 1$ the convergence condition for a unique solution is more restrictive. We then require that as $i \rightarrow \infty$,

$$\nu^i f^*(\eta_0 + i) = e^{i \log(\nu)} f^*(\eta_0 + i) \rightarrow 0 \quad \text{faster than } i^{-1},$$

for which a sufficient condition is $f^*(\eta_0 + i) \sim e^{-ai}$ with $a > \log \nu$. Such exponential decline of f^* is not guaranteed by the physical requirement of finite beam flux or power and is not satisfied by power-law f^* extending to infinite energies. It follows that the solution of (8), with our representation of the real solar ionisation structure, for f is not unique unless f^* and hence the associated photon spectrum has sufficiently rapid exponential decline at high energy. This rather strong condition is satisfied for f^* with a high-energy cut-off and we show below how a unique solution for $f(\eta)$ can be constructed in that case.

This situation can be understood in terms of null functions as follows. The homogeneous solutions, Equation (11), behave as $f_0(\eta_0 + j) = (-\lambda)^j \phi(\eta_0)$. Since

$\nu > 1$ these decline like $e^{-j \log \nu}$ at large η but alternate in sign. If a solution f of (8) declines faster than this, then addition of any null-function solution $\phi(\eta_0)$ in $0 < \eta_0 \leq 1$ would result in unphysical negative values of f at large η . Consequently the physical condition $f \geq 0$ demands that no non-uniqueness be introduced by addition of null-function solutions. In the following we illustrate the situation of non-uniqueness for a specific example where f^* does not decline exponentially.

5.3. EXAMPLE OF PHYSICALLY ACCEPTABLE NON-UNIQUE SOLUTIONS

In analysing conditions on f^* under which physically acceptable solutions for f do exist, and their uniqueness, it is also useful to consider explicit inversion formulae for Equation (8). One such is easily shown to be the Fourier solution

$$f(\eta) = \mathcal{F}^{-1} \left\{ \frac{\tilde{f}^*(\omega)}{1 + \lambda e^{i\omega}}; \eta \right\}, \quad (15)$$

where \tilde{f}^* is the Fourier transform of f^* which is a special case of the Fourier solution of the general problem mentioned in Section 2. Such Fourier solutions are likely to prove useful in numerical treatment of real data but a more useful form for our present analytic study is to consider Laplace transforms, which can prove helpful in solving functional equations (Sneddon, 1972). To obtain a Laplace solution we define $F(s)$ by

$$f(\eta) = \int_0^{\infty} F(s) e^{-s\eta} ds = \mathcal{L}[F(s); \eta],$$

so that $F(s)$ is the inverse Laplace transform of $f(\eta)$, and similarly define $F^*(s)$ in terms of $f^*(\eta)$. It then follows that

$$f(\eta + 1) = \mathcal{L}[e^{-s} F(s); \eta]$$

and on taking the inverse Laplace transform of (8) we obtain

$$F(s) + \nu e^{-s} F(s) = F^*(s) \quad (16)$$

and hence the solution

$$f(\eta) = \mathcal{L} \left[\frac{F^*(s)}{1 + \nu e^{-s}}; \eta \right] = \int_0^{\infty} \frac{\mathcal{L}^{-1}[f^*(\eta); s]}{1 + \nu e^{-s}} e^{-s\eta} ds.$$

This form enables computation of f in cases where $\mathcal{L}^{-1}[f^*(\eta); s]$ exists and hence consideration of existence and physical acceptability for different f^* . Note that for the null solution (11), \mathcal{L}^{-1} does not exist, because of the discontinuities in $f(\eta)$.

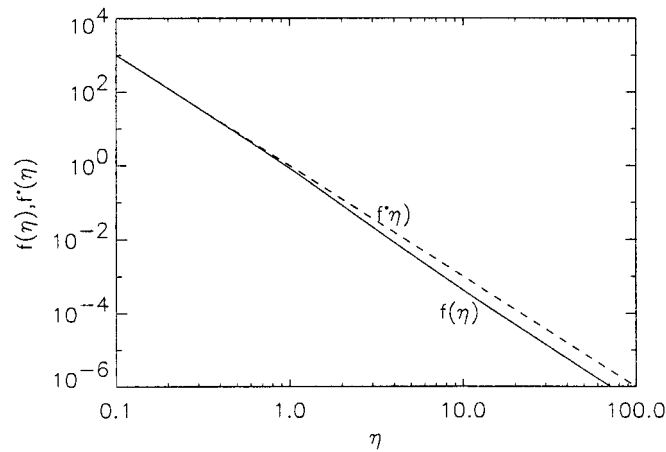


Figure 8. Injection spectrum f required for a step-function-ionized target to yield the same photon spectrum as a pure power-law spectrum f^* injected into an ionized target.

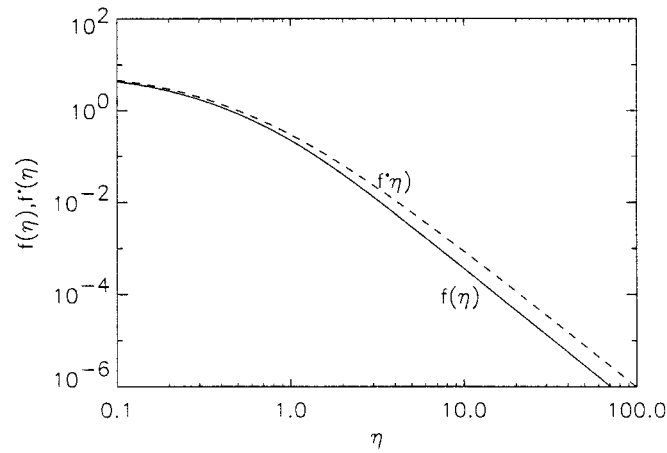


Figure 9. Injection spectrum f required for a step-function-ionized target to yield the same photon spectrum as a displayed power-law spectrum f^* injected into an ionized target.

This may be formally proved by noting that the null solution $f^*(\eta) = 0$ requires $F^*(s) = 0$ and hence, Equation (16) (since $1 + \nu e^{-s} > 0$ for all s) that $F(s) = 0$. Hence the only null solution with an inverse Laplace transform is the trivial case $f(\eta) = 0$.

Some solutions for special forms of f^* , whose inverse Laplace transforms are tabulated, are of interest. First if $f^*(\eta) = e^{-\beta\eta}$, so that $F^*(s) = \delta(s - \beta)$, then

$$f(\eta) = \frac{1}{1 + \nu e^{-\beta}} e^{-\beta\eta},$$

as already found in Section 4 for the forward problem (cf., Figure 3). Second, for a pure power-law $f^*(\eta) = \eta^\alpha$, $F^*(s) = s^{\alpha-1}/\Gamma(\alpha)$ and so

$$f(\eta) = \frac{1}{\Gamma(\alpha)} \int_0^\infty \frac{s^{(\alpha-1)}e^{-s\eta}}{1 + \nu e^{-s}} ds . \tag{17}$$

(This Laplace transform solution to the inverse problem for a power-law $f^*(\eta)$ is precisely the integral definition of the special function ‘ $\Phi(\eta\alpha, s)$ ’ in Gradshtein and Ryzik (1994) who give the equation $f(x) + \nu f(x + 1) = f^*(x)$ as one of the properties of this function, which appears to be related to the Riemann Zeta function.) This is the injection spectrum into a step-function-ionized target needed to produce a pure power-law photon spectrum, as produced in an ionized target by a pure power-law electron spectrum. It is clearly ≥ 0 and has the same properties as f^* , in that $f \rightarrow 0$ as $\eta \rightarrow \infty$ and $f \rightarrow \infty$ as $\eta \rightarrow 0$. Its form is given in Figure 8 for $\alpha = 3$ which shows, as would be expected that f is suppressed relative to f^* at high η by a factor of up to $\lambda + 1$ because of the reduced collisional energy losses there. Third, for the displaced power-law $f^* = (\eta + \eta_0)^{-\alpha}$ (which is more physically realistic since $f^*(0)$ is finite), $F^*(s) = e^{\eta_0 s} s^{\alpha-1}/\Gamma(\alpha)$ and

$$f(\eta) = \frac{1}{\Gamma(\alpha)} \int_0^\infty \frac{s^{(\alpha-1)}e^{-s(\eta+\eta_0)}}{1 + \nu e^{-s}} ds .$$

This solution is non-negative everywhere, remains finite as $\eta \rightarrow 0$, and is shown in Figure 9.

More generally, the solution given in Equation (15) will allow exploration of conditions on f^* for a solution $f \geq 0$. We do not pursue this further here but note that one sufficient (though not necessary) condition is that $F^*(s) > 0$ for all s and consequently (cf., Brown and Emslie, 1989) that

$$\text{Sign of } \left[\frac{d^j f^*(\eta)}{d\eta^j} \right] = (-1)^j .$$

To give a particular example of non-uniqueness of physically acceptable solutions we consider the ‘data’ spectrum

$$f^*(\eta) = \eta^{-\beta} + \nu(\eta + 1)^{-\beta}$$

for which, by design, $f_1(\eta) = \eta^{-\beta}$ is a physically acceptable solution of Equation (8). To this we will add a homogeneous null-function solution of type (11), adopting for simplicity a constant ϕ (recall that $\lambda = \nu^{-1}$),

$$f_0(\eta) = f_0(j + \eta_0) = (-\lambda)^j A \quad \text{for } j < \eta \leq j + 1$$

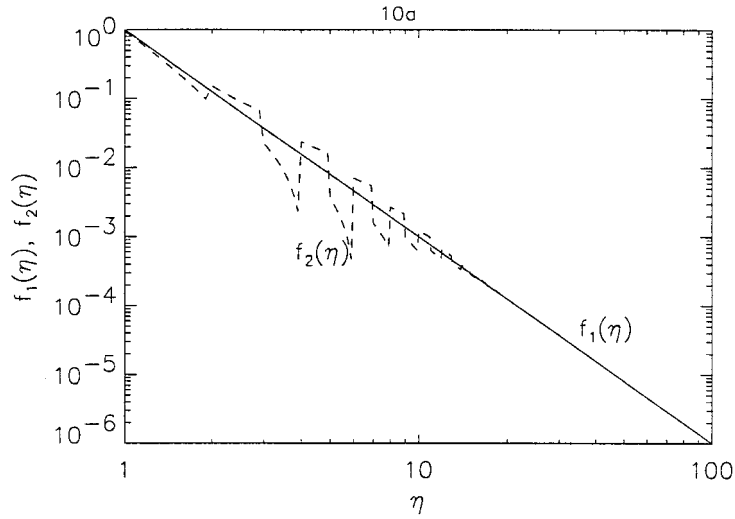


Figure 10a. Two injection spectra f_1 (power-law spectrum), f_2 (power-law plus homogeneous solution with $\Phi = \text{constant}$) which produce precisely the same bremsstrahlung photon spectrum.

(i.e., $\phi(\eta_0) = A$ in $0 < \eta_0 \leq 1$), where A is a constant. Then the sum, f_2 , of $f(\eta) = \eta^{-\beta}$ and $f_0(\eta)$,

$$f_2(\eta) = (j + \eta_0)^{-\beta} + (-\lambda)^j A,$$

is also a solution of (8). This will be physically acceptable provided A is small enough to ensure that $(j + \eta_0)^{-\beta} \geq A\lambda^j$. Now

$$(j + \eta_0)^{-\beta} - A\lambda^j \geq (j + 1)^{-\beta} - A\lambda^j,$$

so a sufficient condition to guarantee $f_2 \geq 0$ is

$$A \leq \nu^j (j + 1)^{-\beta} \tag{18}$$

for all j . Setting to 0 the derivative with respect to j of the right-hand side of (18) yields the maximum permissible value

$$A_{\max} = \frac{1}{\nu} \left[\frac{e \log \nu}{\beta} \right]^\beta$$

such that

$$f_2(\eta) = (j + \eta_0)^{-\beta} + A_{\max} (-\lambda)^j \geq 0$$

for all $\eta \geq 0$.

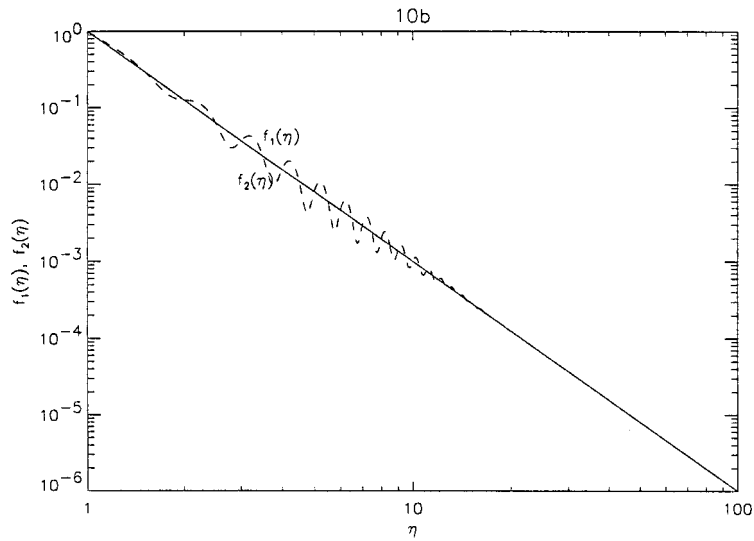


Figure 10b. Two injection spectra f_1 (power-law spectrum), f_2 (power-law plus homogeneous solution with $\Phi = \sin(\eta)$) which produce precisely the same bremsstrahlung photon spectrum. In this case f_2 is continuous and differentiable over all η .

Two injection spectrum f_1 (power-law spectrum), f_2 (power-law plus homogeneous solution with $\Phi = \sin(\eta)$) which produce precisely the same bremsstrahlung photon spectrum. In this case f_2 is continuous and differentiable over all η .

In Figure 10(a) we show one of the infinity of such solutions with $A < A_{\max}$ together with f_1 . Any such spectrum f_2 yields precisely the same photon spectrum from a step-function-ionized target. The example in Figure 10(a) is for a null function which has infinitely many discontinuities at intervals $\Delta\eta = 1$ because $\phi(\eta_0) = \text{constant}$. There is, however, a subset of the null-function f_0 space which is continuous. For continuity Equation (11) requires that $f_0 \rightarrow 0$ at all points where it changes sign. It also requires that f_0 decrease by a factor ν over all intervals $\Delta\eta = 1$. These conditions are satisfied by the form

$$f_0(\eta) = A_k \nu^{-\eta} \sin[(2k + 1)\eta + \eta_k],$$

where k is any integer ≥ 0 , and A_k, η_k are arbitrary phase and amplitude, or more generally by

$$f_0(\eta) = \sum_{k=0}^{\infty} A_k \nu^{-\eta} \sin[(2k + 1)\eta + \eta_k].$$

In Figure 10(b) we show an example of this where we have added to the smoothed power-law solution the null function with the lowest frequency component ($k = 0$) only and with A_k, η_k chosen so that the sum is non-negative everywhere. This

shows that the non-uniqueness occurs through the action of the kernel on the bremsstrahlung spectrum to filter out completely all damped harmonic components in the electron spectrum $f(\eta)$ with ‘frequencies’ which are odd multiples of that associated with the transition zone depth energy E_1 .

It is important to realise that the non-uniqueness involved here is of a very serious type and is far more than just the inability to resolve small-scale features that is commonly encountered in inverse problems in astrophysics (and elsewhere). For example, it is frequently the case with continuous inverse problems such as image reconstruction that discrete sampling (not to mention data errors) renders the small-scale features in the image unrecoverable – in other words there is a lack of resolution. In practice, the use of some kind of regularisation (cf., Craig and Brown, 1986) permits extraction of information about larger-scale features that is contained in the data. In the inverse problem described, this lack of resolution is also present but the non-uniqueness of the solution is a much more fundamental limitation. There can exist many distinct exact solutions to the inverse problem (Equation (8)) (for a given data spectrum $f^*(\nu)$) that differ by much more than just small-scale features. For example, two exact solutions such as in Figure 10, differing by a null function, obviously do not differ only by short-wavelength variations. The null function will contain some periodic variation of period $\Delta\eta = 1$ on top of the $\nu^{-\eta}$ trend, corresponding to variations in the electron spectrum over an energy range equal to $E_1 \sim 30$ keV which is certainly not a small-scale variation in the solution. Furthermore, there is nothing about these solutions that in any way marks them out as pathological or non-physical, that would permit one particular solution to be singled out as being physically more reasonable.

5.4. SPECTRAL CUT-OFFS AND UNIQUE SOLUTIONS

In the above three examples $f^*(\eta)$ is non-zero everywhere. New interesting features of the solution of (8) arise for cases where $f^*(\nu) = 0$ in some range. Suppose that $f^*(\eta) = 0$ for $\eta < \eta_1$. Then

$$f(\eta) + \nu f(\eta + 1) = 0 \quad \text{in} \quad 0 < \eta < \eta_1$$

which in order for f to be ≥ 0 requires that

$$f(\eta) = 0 \quad \text{in} \quad 0 < \eta < \eta_1 \quad \text{and in} \quad 1 < \eta < \eta_1 + 1 .$$

For $\eta_1 < 1$ this implies that $f(\eta)$ has, like f^* , a cut-off below η_1 , but has, in addition, a gap, i.e., $f = 0$ in the range $1 < \eta < \eta_1 + 1$. For $\eta_1 > 1$, the two ranges overlap and f has a lower cut-off at $\eta = \eta_1 + 1$. (The latter corresponds to a cut-off in $F_0(E_0)$ at $E_0 = E_c = (E_c^{*2} + E_1^{*2})^{1/2}$, where E_c^* is the cut-off energy in F_0^* corresponding to η_1 .) This argument can then be applied to successive intervals of η to yield a recursive solution for f . Considering again the case $\eta_1 > 1$ we have by (8), since $f(\eta) = 0$, for $\eta < \eta_1 + 1$,

$$\lambda[f^*(\eta) - f(\eta)] = \lambda f^*(\eta), \quad \text{where } \eta_1 < \eta < \eta_1 + 1,$$

which defines f in $\eta_1 + 1 < \eta < \eta_1 + 2$. Repeating this processes yields

$$f(\eta + j) = - \sum_{i=0}^{j-1} (-\lambda)^{j-i} f^*(\eta + i),$$

which allows computation of f from f^* . We show results in Figures 11(a–c) for power laws in f^* with $\alpha = 3$ and cut-offs at $\eta_1 = 1, 2, 5$, respectively, and in Figures 12(a–c) with $\alpha = 4$ and same η_1 values. It is clear that physically acceptable solutions for f (≥ 0) exist only for sufficiently large η_1 , the actual value depending on α . In addition we note that, even when $f \geq 0$ the solution is oscillatory and highly structured (with infinitely many discontinuities) which seems physically implausible. This means that many photon spectra which can be produced by reasonable f^* in a fully-ionized target cannot be produced by a ‘physically plausible’ f in a plasma with ionisation structure like the solar atmosphere. The reason that we are able to obtain a unique solution here is that specifying $f^*(\eta) = 0$ over a non-zero range demands that $f(\eta) = 0$ over a range sufficient to eliminate the possibility of adding non-zero homogeneous solutions ϕ .

Secondly if f^* has an upper cut-off at η_2 we can construct a recursive solution starting at high η . That is, since $f(\eta) = 0$ for $\eta > \eta_2$ then in $\eta_2 - 1 < \eta < \eta_2$ we have $f(\eta) = f^*(\eta)$, etc., to give

$$f(\eta_2 - j + \Delta\eta) = \sum_{i=0}^{j-1} \left(\frac{-1}{\lambda}\right)^i f^*(\eta_2 - i + \Delta\eta),$$

where $j, \Delta\eta$ are the integer and fractional parts of η_2 .

6. Bounds on $f(n)$ and on Total Beam Electron and Energy Fluxes

First we note that inequalities (13) can be used, for any particular form of $f^*(\eta)$, to put upper and lower bounds on the forms of $\Phi(\eta_0)$ (and hence of $f(\eta)$) consistent with $f(\eta) \geq 0$ everywhere. This is likely to be useful in practice and we will explore its application in future work.

Also important are the total beam injection rate and power. An obvious limit on any non-negative solution of (8) is $f(\eta) \leq f^*(\eta)$ – i.e., no acceptable solutions for f can exceed the fully-ionized solution f^* anywhere. It has already been noted that inference of the wrong shape for the electron injection spectrum, by use of incorrect target ionisation structure, can lead to mis-diagnosis of the acceleration process and incorrect inference (usually exaggeration) of the total beam flux and power by extrapolation of an incorrect spectral shape. If complete information is available

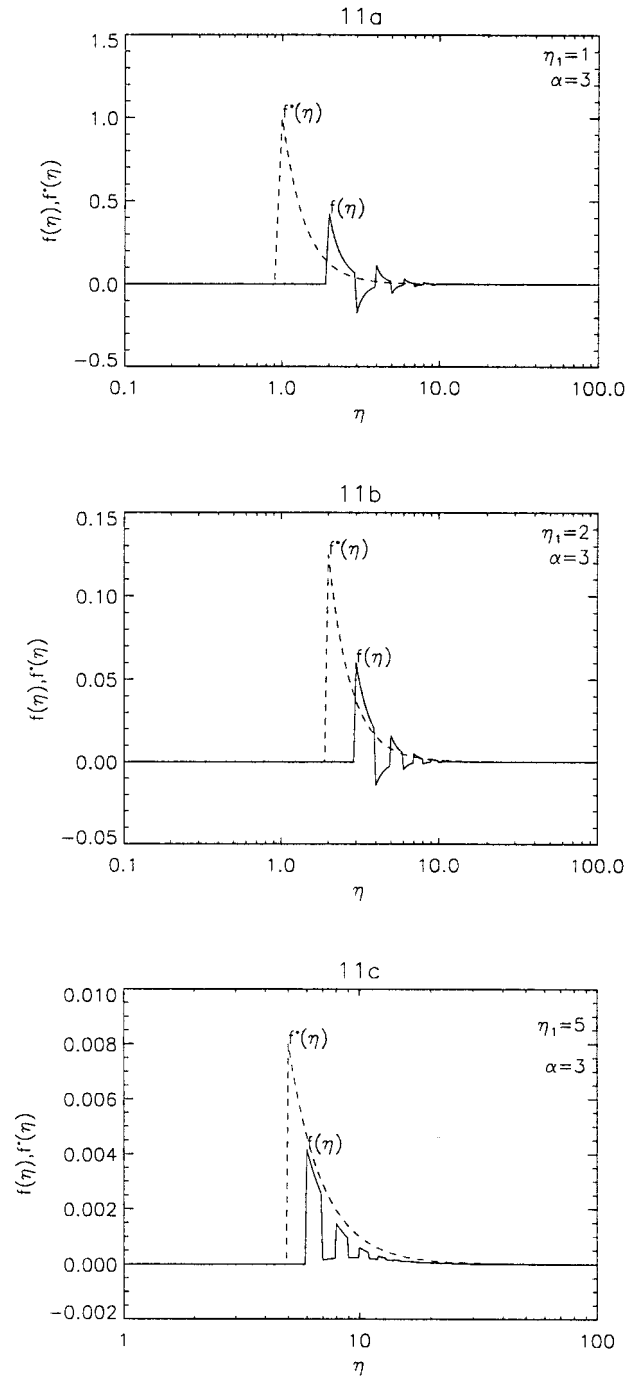


Figure 11. Injection spectrum f required for a step-function-ionized target to yield the same photon spectrum as a power-law spectrum with low cut-off f^* at η_1 injected into an ionized target, for $\alpha = 3$ and various η_1 values.

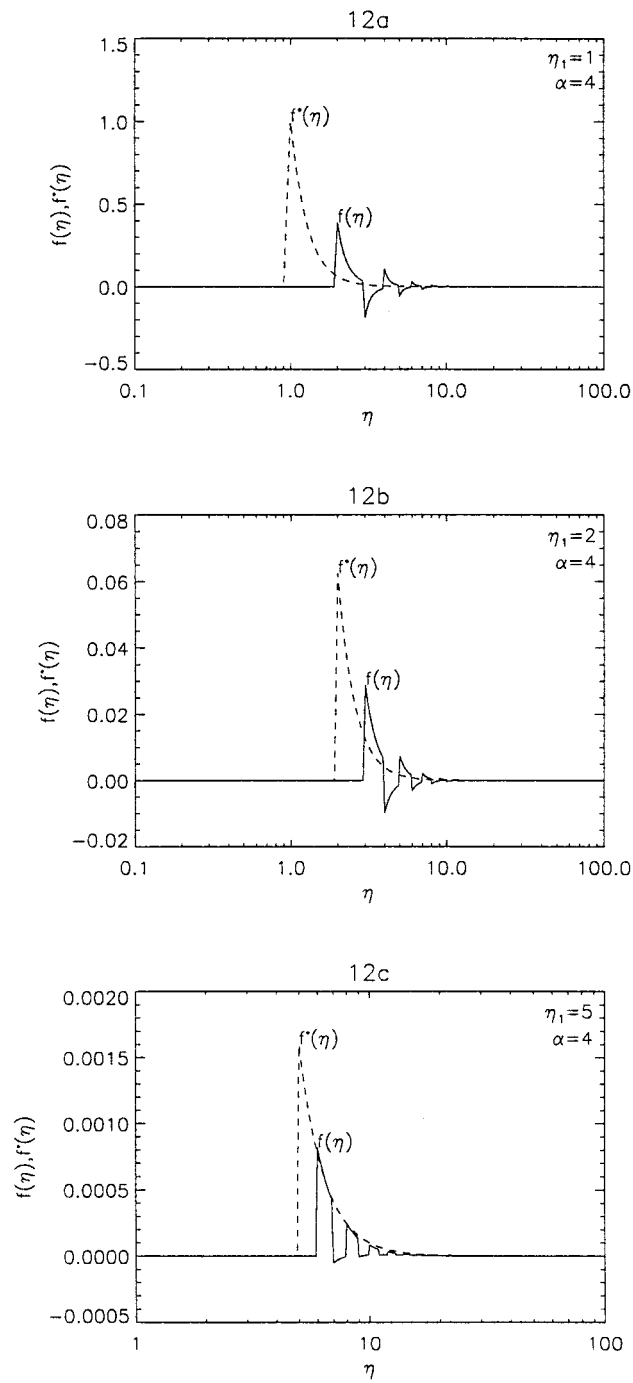


Figure 12. Injection spectrum f required for a step-function-ionized target to yield the same photon spectrum as a power-law spectrum with low cut-off f^* at η_1 injected into an ionized target, for $\alpha = 4$ and various η_1 values.

over the whole spectral range and if we use the correct ionisation structure, this should in principle be avoidable. Integration of Equation (8) yields the total electron number and energy fluxes required in the two models (target configurations) needed to give the same photon spectrum. The total (scaled) electron fluxes f_{tot} are given by $\int_0^\infty f \, d\eta$ (and similarly for f_{tot}^*), so by (8)

$$f_{\text{tot}} = \frac{\lambda}{\lambda + 1} f_{\text{tot}}^* + \frac{1}{\lambda + 1} \int_0^1 f(\eta) \, d\eta \geq \frac{\lambda}{\lambda + 1} f_{\text{tot}}^*, \quad (19)$$

so that, in terms of electron numbers (directly inferred, rather than extrapolated) the step-function-ionized target can never require fewer electrons than the fraction $\lambda/(\lambda + 1)$ of the number required for a fully ionized target. A surprising result is that if f has a lower cut-off at $\eta_1 \geq 1$ the electron number reduction factor is always precisely $\lambda/(\lambda + 1)$ (since the integral term in (19) is zero) regardless of the shape of f above the cut-off. The total (scaled) electron energy fluxes (powers) P are given by $\int_0^\infty f \eta^{1/2} \, d\eta$ (and similarly for P^* in terms of f^*), so by (8)

$$P = P^* - \frac{1}{\lambda} \int_1^\infty f(\eta) (\eta - 1)^{1/2} \, d\eta. \quad (20)$$

If f is non-zero only in $\eta \leq 1$ then of course $P = P^*$ since all the bremsstrahlung is produced in the ionized region of the target. If f is concentrated at η close to, but partially above, $\eta = 1$ then P approaches the value P^* . If f is concentrated at $\eta \gg 1$ then the integral term in (20) approaches P/λ and we get $P \rightarrow P^* \lambda/(\lambda + 1)$. These values of P/P^* represent the extremes of the possible range which are the same as those for $f_{\text{tot}}/f_{\text{tot}}^*$.

7. Discussion and Conclusions

We have shown that the electron injection spectrum required to yield a given bremsstrahlung spectrum in a thick target depends crucially on the form of the ionisation structure of the target. We have found the very important result that physically acceptable solutions for the case with ionisation structure may not exist or may be non-unique (even though unique acceptable solutions exist for the fully ionized case), unless the electron spectrum in the latter has a low-energy cut-off or a rapid decline at high energies. For cases where such cut-offs do exist we have obtained summation expressions determining the unique solution for the case with target ionisation structure. In our analysis we have mainly compared a fully ionized target with one of step function ionisation structure as an example approximating the solar transition zone structure relevant to flares. Even in the case of smooth electron spectra, the shape differs significantly between the two, especially for energies just

above the electron energy required to reach the transition zone, because of the reduction in collisional losses there. For injection spectra containing sharp features, the two target models can give very different answers, even when these are unique. Solutions for an ionized target, typically used for data analysis, generally contain spurious electrons at low energies. Thus particular caution has to be exercised for results where a low-energy electron cut-off is expected or appears to be present in results obtained using ionized-target formulae such as the thick-target analysis by Johns and Lin (1992) of data with a ‘superhot’ component (Lin and Schwartz, 1987) subtracted. When the spectral range of the non-thermal bremsstrahlung data covered is incomplete, due to instrument bandwidth or overlap of a ‘superhot’ component at low energies, these erroneous inferences at low energies are likely to lead to exaggerated estimates of total electron flux by extrapolation of the incorrect spectrum. It is therefore important for future high-resolution HXR spectrometry that inversion methods be developed to include target ionisation structure along the lines discussed above. Obvious improvements over our analysis will be inclusion of a smoother fall in ionisation with depth than we have used in most of our analysis and of a more accurate bremsstrahlung cross-section than Kramers.

Another important feature is that almost all of our results have been discussed in terms of $\eta = (E_0/E_1)^2$ rather than of energy E_0 itself, E_1 being taken as known. In practice E_1 will not be well known, depending on the column depth of the transition zone. However, if we have any independent estimates of or bounds on $F_0(E_0)$, accurate measurements of the HXR spectrum will enable us to estimate E_1 and hence the depth of the transition zone and potentially how it evolves with time through chromospheric evaporation. Even just the requirement that the inversion should yield $F_0(E_0) \geq 0$ may suffice to constrain E_1 on which we have shown the form of solution to depend.

A natural question to ask is whether the non-uniqueness we have established could be an artefact of our approximation of the transition zone as a discontinuity in $x(M)$, i.e., in $k(\zeta)$, where $\zeta = (\eta - \xi)$ as before (Equation (7)). A more realistic form would be to take $k(\zeta)$ as a linear ramp up from $k = 1/(\lambda + 1)$ at $\zeta = 1$ to $k = \lambda^{-1}$ at $\zeta = 1 + \Delta$, where Δ is a finite transition zone thickness. It is straightforward to show that Equation (8) is then replaced by

$$f(\eta) + \nu f(\eta + 1) + \left[\nu \int_{\eta+1}^{\eta+1+\Delta} \frac{f(\eta') d\eta'}{\Delta} - f(\eta + 1) \right] = f^*(\eta). \quad (21)$$

The ‘correction’ to Equation (21) in the [...] term of this equation amounts to the contribution to f^* of the bremsstrahlung emission in the transition zone, which will be very small unless $f(\eta')$ is nearly singular at $\eta + 1$ (i.e., is a delta function or is concentrated in a range of $\eta \leq \Delta$ around $\eta + 1$). Since the transition region is very thin, we can rule this out and infer that our conclusions concerning non-uniqueness are effectively unchanged.

Acknowledgements

We gratefully acknowledge the financial support of NASA's Space Physics Division and of a PPARC Visitor Grant (AGE), Rolling Research Grant (JCB) and Studentship (GMcA) and of a NATO Collaborative Research grant. The work benefited from discussions with A. Wood.

References

- Brown, J. C.: 1971, *Solar Phys.* **18**, 489.
Brown, J. C.: 1972, *Solar Phys.* **26**, 441.
Brown, J. C.: 1973, *Solar Phys.* **28**, 151.
Brown, J. C.: 1975, in S. R. Kane (ed.), 'Solar Gamma-, X-Ray, and EUV Radiation', *IAU Symp.* **68**, 245.
Brown, J. C. and Emslie, A. G.: 1988, *Astrophys. J.* **331**, 554.
Brown, J. C. and MacKinnon, A. L.: 1985, *Astrophys. J.* **292**, L31.
Craig, I. J. D. and Brown, J. C.: 1986, *Inverse Problems in Astronomy*, Hilger, Bristol.
Emslie, A. G.: 1978, *Astrophys. J.* **224**, 941.
Gradshteyn, I. S. and Ryzhik, I. M.: 1994, *Tables of Integrals, Series and Products*, Academic Press, New York.
Johns, C. and Lin, R. P.: 1992, *Solar Phys.* **137**, 121.
Judge, P., Hubeny, V., and Brown, J. C.: 1997, *Astrophys. J.*, in press.
Kuczma, M.: 1968, *Functional Equations in a Single Variable*, Polska Akademia Nauk, Monografie Matematyczna, vol. 46, PWN-Polish Scientific Publishers.
Lin, R. P. and Schwartz, R.: 1987, *Astrophys. J.* **312**, 462.
MacKinnon, A. L. and Brown, J. C.: 1989, *Astron. Astrophys.* **215**, 371.
Piana, M.: 1994, *Astron. Astrophys.* **288**, 949.
Santangelo, N.: 1973, *Solar Phys.* **29**, 143.
Thompson, A. M., Craig, I. J. D., Brown, J. C., and Fulber, C.: 1992, *Astron. Astrophys.* **265**, 278.
Tomblin, F. F.: 1972, *Astrophys. J.* **171**, 377.